European Journal of Medicinal Chemistry 45 (2010) 2860–2867

Contents lists available at ScienceDirect

European Journal of Medicinal Chemistry

journal homepage: http://www.elsevier.com/locate/ejmech

Original article

Synthesis and structure-activity relationship study of 8-hydroxyquinoline-derived Mannich bases as anticancer agents

Arthur Y. Shaw [a,e,*], Chun-Yi Chang [a], Mei-Yuan Hsu [a], Pei-Jung Lu [b], Chia-Ning Yang [c], Hui-Ling Chen [b], Cheng-Wei Lo [c], Chung-Wai Shiau [d], Ming-Kai Chern [a]

[a] Department of Chemistry, Tamkang University, Danshui 251, Taiwan
[b] Institute of Clinical Medicine, National Cheng Kung University, Tainan 701, Taiwan
[c] Institute of Biotechnology, National University of Kaohsiung, Kaohsiung 700, Taiwan
[d] Institute of Biopharmaceutical Sciences, National Yang-Ming University, Taipei 112, Taiwan
[e] Department of Pharmacology and Toxicology, College of Pharmacy, The University of Arizona, Tucson, AZ 85724, USA

ARTICLE INFO

Article history:
Received 15 October 2009
Received in revised form
4 March 2010
Accepted 9 March 2010
Available online 12 March 2010

Keywords:
Clioquinol
8-Hydroxyquinoline
Mannich-type reaction
Structure-activity relationship

ABSTRACT

To continue our early study on the structural modifications of clioquinol, more 8-hydroxyquinoline-derived Mannich bases were synthesized and examined for growth-inhibitory effect. Taken Mannich base **1** as our lead compound, upon replacement of either sulfonyl group with methylene group or piperazine ring with ethylenediamine group resulted in an appreciable increase in potency. On the other hand, as 8-hydroxyquinoline was replaced with phenol, 3-hydroxypyridine and 1-naphthol, a dramatic decrease in activity was observed, indicating that 8-hydroxyquinoline is a crucial scaffold for activity. Further 3D-QSAR analysis on HeLa cells revealed that both steric and electronic effects contributed equally to growth inhibition. Taken together, the structure-activity relationships obtained from both *in vitro* data and CoMFA model warrant a valuable reference for further study.

1. Introduction

In addition to applications in the design of chemosensors and optical devices [1–4], 8-hydroxyquinoline has been synthesized with a variety of biological activities, such as inhibitors of catechol *O*-methyltransferase [5], inhibitors of HIF-1α prolyl hydroxylase [6], inhibitors of HIV-1 integrase [7], antibacterial [8,9], antimalarial [10], and antitumor agents [11–13]. Similar to carbonyl compounds with keto-enol tautomerism that enables a multiple-component Mannich reaction, 8-hydroxyquinoline can be carried out to generate the corresponding Mannich bases [10,14,15]. As a consequence, several Mannich bases of 8-hydroxyquinoline derivatives have been synthesized to show several biological activities [16,17].

On the other hand, clioquinol (5-chloro-7-iodo-8-hydoxyquinoline, Fig. 1) was clinically used as an antibiotic for the treatment of diarrhea and skin infection. Recently, clioquinol has demonstrated to exhibit anti-Alzheimer's disease in a mouse model via the reduction or prevention of amyloid plaque accumulation in the brain [18,19]. Apart from its antibiotic and anti-Alzheimer's disease efficacies, clioquinol also showed a moderate antiproliferative effect on cancer cells. The mechanistic study revealed that clioquinol-induced antiproliferative effect is attributed to caspase-dependent apoptotic pathway. Moreover, antiproliferative effect mediated by clioquinol could be enhanced in the presence of metal ions thanks to its metal-binding property [20,21].

Our early study showed that upon the elongation of 8-hydroxyquinoline appended by an arylsulfonylpiperazine moiety (**1** and **25**, Fig. 1) through Mannich-type reaction resulted in dramatically improved growth-inhibitory effect. We further demonstrated that growth inhibition induced by 8-hydroxyquinoline-derived Mannich bases was attributed to caspase-dependent apoptotic pathway and generation of oxygen reactive species. The synergistic effect of growth inhibition mediated by Mannich bases was also observed in the presence of copper ion, which was in accordance with that of clioquinol [22]. Herein, we would like to report the structural modifications of 8-hydroxyquinoline-derived Mannich bases with aim to examine their growth-inhibitory effect. Moreover, 3D-QSAR analysis employed by CoMFA model on HeLa cell line will be presented in this paper as well.

2. Chemistry

As shown in Fig. 2, a series of 8-hydroxyquinoline-derived Mannich bases were prepared in a systematic manner. In Route A,

* Corresponding author. Tel.: +886 2 2621 5656; fax: +886 2 2620 9924.
E-mail address: shaw.299@gmail.com (A.Y. Shaw).

0223-5234/$ – see front matter © 2010 Elsevier Masson SAS. All rights reserved.
doi:10.1016/j.ejmech.2010.03.008

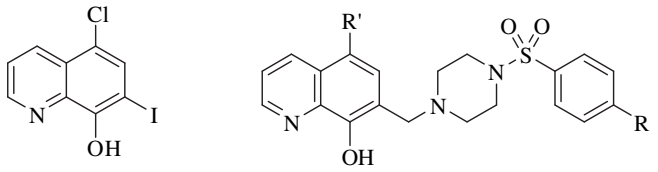

Fig. 1. Chemical structures of clioquinol and its Mannich bases **1** and **25**.

we replaced a variety of substituents on benzene ring to obtain **2**–**17** (Scheme 1, Fig. 3). In Route B, the sulfonyl group was replaced by either a carbonyl group or a methylene group to generate **18** and **19**, respectively (Scheme 2, Fig. 3). In Route C, the piperazine moiety in **1** was replaced by an ethylenediamine linker to synthesize **20** (Scheme 3, Fig. 3). In Route D, Mannich-type reaction of hydroxyarenes such as phenol, 3-hydroxypyridine, 1-naphthol and 5-subsituted 8-hydroxyquinoline were utilized to afford **21**–**27** (Scheme 4, Fig. 3, Table 1). Accordingly, a mixture of hydroxyarene, along with formaldehyde and amine was stirred in ethanol at reflux for 16–22 h that successfully prepared the corresponding Mannich bases [10,14,15,22].

3. Results and discussion

All tested compounds were screened on a panel of human carcinoma cell lines for growth-inhibitory activities, including HeLa (cervical epithelioid carcinoma cell), BT483 (mammary gland adenocarcinoma cell), SKHep (hepatocellular carcinoma cell) and CE81T (esophageal carcinoma cell). The MTT (3-[4,5-dimethylthiazol-2-yl]-2,5-diphenyltetrazolium bromide) assay [23] was employed for the growth inhibition studies and the GI_{50} values are summarized in Tables 2 and 3. The compound concentration causing a 50% cell growth inhibition (GI_{50}) was determined by interpolation from dose-response curves.

As compared to **1** (phenyl, GI_{50}, 6.8 μM), **5** (4-methylphenyl, GI_{50}, 2.5 μM), **6** (4-isoprpylphenyl, GI_{50}, 6.1 μM), **7** (4-*tert*-butylphenyl, GI_{50}, 4.7 μM) and **8** (4-biphenyl, GI_{50}, 4.5 μM), both **16** and **17** bearing 1-naphthyl and 2-naphthyl moieties exhibited higher growth-inhibitory effect against HeLa cells with GI_{50} values of 1.8 and 1.7 μM, respectively. These results indicate a certain degree of planar geometry in aromatic system connected to the sulfonyl group is favorable for growth-inhibitory activity. On the other hand, data showed that either electron-donating substituents such as **5** (4-CH_3, GI_{50}, 2.5 μM) and **10** (3-OMe, GI_{50}, 2.4 μM) or electron-withdrawing substituents like **9** (4-CF_3, GI_{50}, 2.2 μM) and **15** (4-NO_2, GI_{50}, 2.3 μM) revealed better activities than the counterpart **1** (GI_{50}, 6.8 μM) against HeLa cells. Interestingly, **10** (GI_{50}, 2.4 μM) bearing 3-methoxy group exhibited higher activity than the counterparts **11** (4-OMe, GI_{50}, 5.0 μM), **12** (3, 4-*di*-OMe, GI_{50}, 5.0 μM) and **13** (4-OCF_3, GI_{50}, 4.3 μM) against HeLa cells. Likewise, the abovementioned structure-activity relationship was also found in both BT483 and SKHep cells. As shown, **10** (3-OMe, GI_{50}, 4.1 μM) showed 3-fold more potent than **12** (GI_{50}, 17.4 μM) against SKHep cells. In addition, the growth inhibition of *mono*-substituted benzene ring in Mannich bases such as **10** (3-OMe, GI_{50}, 7.2 μM) and **11** (4-OMe, GI_{50}, 5.2 μM) revealed higher activity than the *di*-substituted counterpart **12** (3, 4-*di*-OMe, GI_{50}, 12.1 μM) against CE81T cells. These findings suggest a distinct steric effect stemmed from the substituted benzene ring that counts for the growth-inhibitory activity. Nevertheless, the electron-withdrawing substituent such as **14** and **15** bearing a nitro group on the benzene ring exhibited a comparable growth-inhibitory activity against all four cell lines. On the other hand, only SKHep showed a higher sensitivity in response to halogen-substituted Mannich bases **2** (4-F, GI_{50}, 4.8 μM), **3** (4-Cl, GI_{50}, 5.0 μM) and **4** (4-Br, GI_{50}, 12.7 μM) as compared to their counterpart **1** (GI_{50}, 14.6 μM). Among analogs modified in Route A, **13** (4-OCF_3) exhibited the most potent growth-inhibitory activity with a GI_{50} value of 2.9 μM against CE81T cell line.

As shown in Scheme 2, upon replacement of the sulfonyl group in **1** with a carbonyl group (**18**) and a methylene group (**19**) resulted in an interesting structure-activity correlation. For example, **19** showed 2- to 10-fold more potent than the counterparts **1** and **18** against four carcinoma cells (Table 3), suggesting the flexibility originated from the rotational methylene group plays a significant role for activity. In addition, **19** exhibited higher potency with a GI_{50} value of 2.6 μM against SKHep cells while both **1** and **18** merely showed moderate activities with GI_{50} values of 14.6 and 26.6 μM, respectively. Unlike **19** bearing a methylene group for free rotation, both **1** (sulfonyl group) and **18** (carbonyl group) are devoid of the rotation capability for activity. Interestingly, as the piperazine ring in **1** was replaced with an ethylenediamine group to generate **20**, an improved growth-inhibitory effect was also observed. Together, these results indicate that the flexible fragments in both **19** and **20**

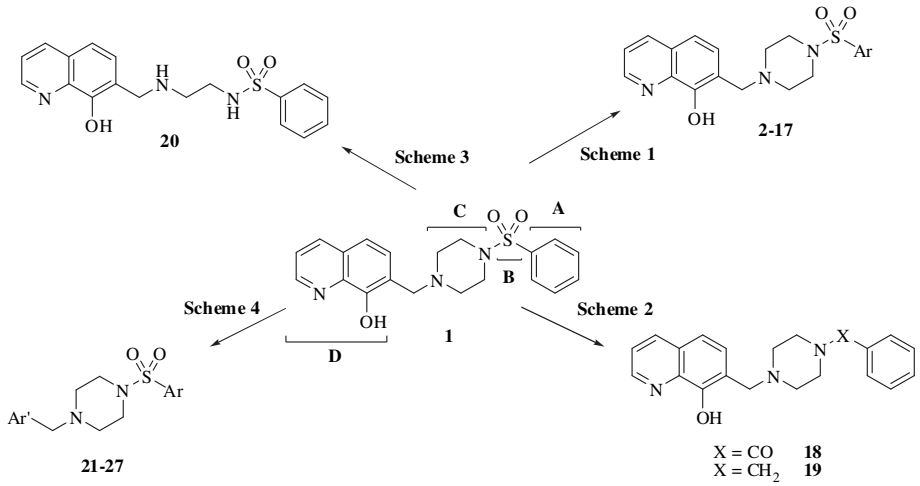

Fig. 2. Overall synthetic routes of structure-activity relationship study of 8-hydroxyquinoline-derived Mannich bases.

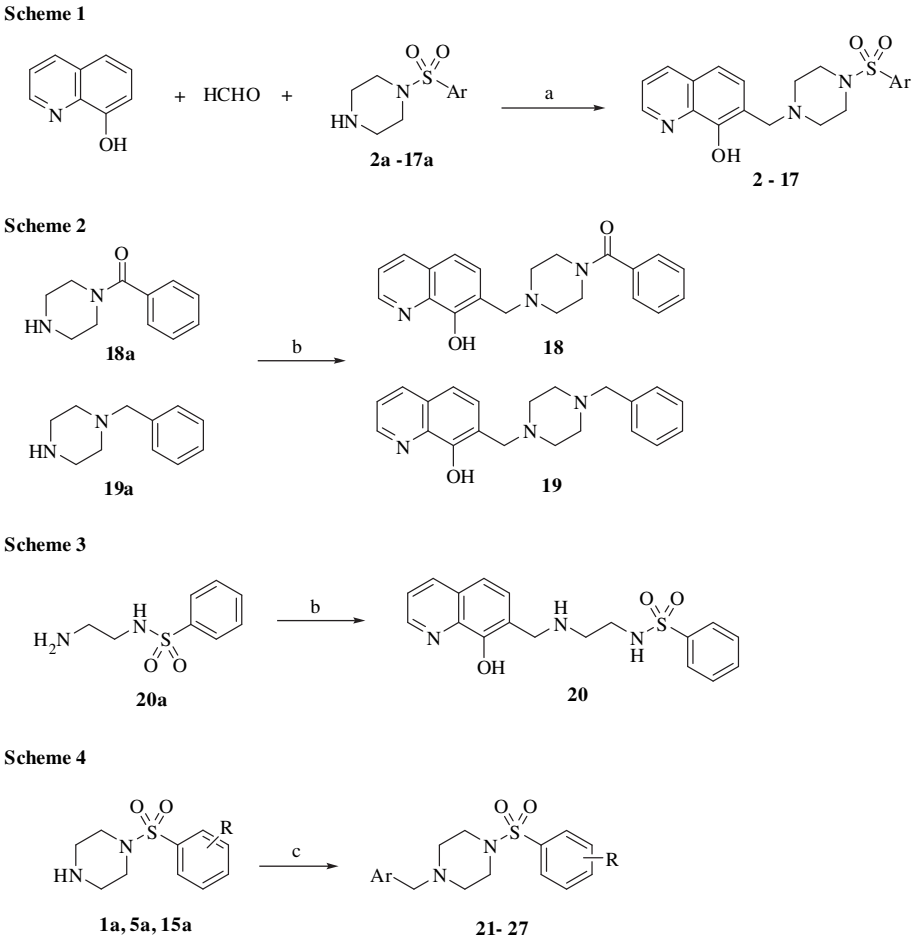

Fig. 3. Synthetic schemes employed for the structure-activity relationship of 8-hydroxyquinolines.

play an important role for growth-inhibitory activity. Consequently, **20** showed more potent activity than their counterpart **1** against both HeLa and SKHep cells with GI_{50} values of 1.4 and 3.6 μM, respectively.

Upon replacement of 8-hydroxyquinoline with phenol, 3-hydroxypyridine, and 1-naphthol (Tables 1 and 3) to obtain the corresponding Mannich bases **21**, **22** and **23**, respectively, all of which exhibited a dramatic loss of activity against screened cell lines, suggesting that 8-hydroxyquinoline is a critical pharmacophore for growth-inhibitory activity. As regard to the modification at 5-position on 8-hydroxyquinoline, Mannich bases **24**–**27** were synthesized that showed a certain degree of structure-activity correlation. For example, exposure of both HeLa and BT483 cells to **24** (5-NO_2 on 8-hydroxyquinoline) exhibited a 2-fold activity as compared to the counterpart **1** (Table 3). Further structural modifications of **24** on the benzene to generate both **25** (4-CH_3) and **26** (4-NO_2) displayed an interesting cell type–selective activity. As shown, both **25** and **26** revealed improved growth-inhibitory effect on HeLa cells in comparison to **24** (GI_{50}, 3.1 μM) with GI_{50} values of 0.7 and 1.2 μM, respectively. Nevertheless, only **25** exhibited 2-fold more potency than **24** against BT483 cells with a GI_{50} value of 1.9 μM, representing the most activity among all tested compounds. Interestingly, among four analogs **24-27**, only **27** bearing 5-chloro group showed 1.6-fold more potent than the parent compound **1** with a GI_{50} value of 5.5 μM against SKHep cells, indicating the preferred sensitivity of individual cell lines in response to the tested compounds.

4. 3D-QSAR on HeLa cell line

To highlight the structure-activity relationship of growth inhibition between carcinoma cells in response to the Mannich bases, CoMFA (Comparative Molecular Field Analysis) was performed by Sybyl 8.1 (Tripos International, 1699 South Hanley Rd., St. Louis, Missouri, 63 144, USA) to build a 3D-QSAR model. The study of HeLa cell line was chosen owing to its significant structure-activity sensitivity toward the tested compounds. The Gasteiger-Huckel method was employed to assigning charges on the Mannich bases and to applying 10 000 steps in Powell algorithm for geometry optimization. A core structure specified in ball and stick was fixed upon constructing the tested compounds (Fig. 4A). The alignment of compounds plays an essential role in determining structure-activity relationship. For the binding site is not available at this stage, we assumed each compound would adopt a conformation in its lowest energy. Database alignment protocol in Sybyl 8.1 was used to align the structures according to the abovementioned core. To build a CoMFA model, the CoMFA descriptors including steric (Lennard-Jones 6–12 potential) and electrostatic (Coulombic potential) field energies were calculated with a sp^3 carbon atom carrying +1.0 charge to serve as a probe atom using Sybyl default parameters.

All compounds were included in training set to build a CoMFA model whose statistical results are listed in Fig. 4B. The optimal number of components (ONC = 6) was recommended after a leave-one-out cross-validated run with q^2 = 0.396, which is

Table 1
Chemical structures of Mannich bases 21–27.

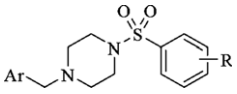

Entry	Ar	R
21	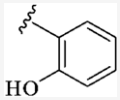	H
22	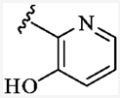	H
23	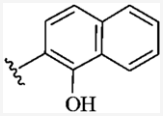	H
24	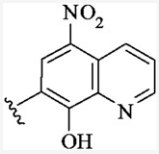	H
25	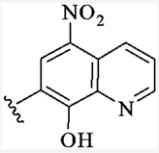	4-CH_3
26	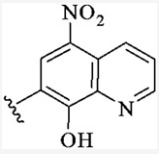	4-NO_2
27	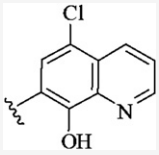	H

acceptable for a small group. The final training set model and coefficients such as R^2 and F-value were obtained by using the optimal number of components and all the data points in the training set. The subsequent non-validation $R^2 = 0.978$ is higher than the criteria value 0.6 required for a fairly good model for more realistic communication that a weak relationship is observed. The subsequent non-validation $R^2 = 0.978$ is higher than the criteria value 0.6 required for a fairly good model. To further ensure the predictive ability of the CoMFA model built by the training set, we carried out a series of test modeling Pred-1, -2, -3, and -4 columns in Fig. 4B by randomly deleting three data point from the training set to generate new models and thus predict the deleted compounds' pIC_{50} values. The test set predictions are given in bold in each Pred-column. Comparing the training and test set results, we found that the fractions of steric and electrostatic contributions to each model are similar and equally important.

CoMFA model presented in Fig. 4A showed all generated fields mapped onto the structure of **25**, the most potent Mannich base in HeLa cell line analysis. As predicted, most of fields sit around the benzene ring system adjacent to the sulfonyl group since a number of modifications are centered in this region. The steric fields on the left side of Fig. 4A indicate that groups such as methyl, trifluoromethyl, and nitro (in **5**, **9**, **15**, **25**, and **26**) bounded to the carbon atom para to the sulfonyl group boost the potency since they fit the green contour (favor bulk group) and bypass the yellow contour (disfavor bulk group). On the contrary, larger groups such as isopropyl and *tert*-butyl in **6** and **7** would contact the yellow contour and lower the potency. Moreover, the abovementioned

Table 2
Growth inhibition of 8-hydroxyquinolines **1-17** against carcinoma cell lines. GI_{50} values are presented as the mean ± sem (standard error of the mean) from four to six separated experiments.

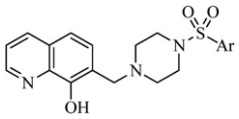

Entry	Ar	GI_{50} (μM)			
		HeLa	BT483	SKHep	CE81T
1	phenyl	6.8 ± 1.1	10.7 ± 2.6	14.6 ± 3.6	5.6 ± 1.8
2	4-fluorophenyl	4.4 ± 0.7	12.5 ± 2.5	4.5 ± 0.5	7.2 ± 0.7
3	4-chlorophenyl	4.6 ± 0.8	12.1 ± 1.8	5.0 ± 0.6	6.0 ± 0.7
4	4-bromophenyl	6.8 ± 0.6	9.0 ± 1.7	12.7 ± 1.9	5.9 ± 0.5
5	4-methylphenyl	2.5 ± 0.2	9.8 ± 1.1	14.3 ± 0.4	4.9 ± 0.9
6	4-isopropylphenyl	6.1 ± 0.5	12.2 ± 0.3	13.8 ± 1.5	7.1 ± 1.5
7	4-tert-butylphenyl	4.7 ± 1.6	11.0 ± 3.2	4.4 ± 0.3	3.3 ± 0.2
8	4-biphenyl	4.5 ± 0.9	11.4 ± 3.8	4.8 ± 0.7	7.0 ± 2.3
9	4-trofluorophenyl	2.2 ± 0.4	5.6 ± 0.5	12.3 ± 1.4	6.2 ± 0.6
10	3-methoxyphenyl	2.4 ± 0.4	6.6 ± 0.5	4.1 ± 1.0	7.2 ± 1.1
11	4-methoxyphenyl	5.0 ± 0.6	11.9 ± 2.1	6.8 ± 0.1	5.2 ± 0.1
12	3,4-dimethoxyphenyl	4.9 ± 0.7	15.5 ± 0.7	17.4 ± 1.0	12.1 ± 3.5
13	4-trifluoromethoxyphenyl	4.3 ± 0.1	7.5 ± 0.6	8.1 ± 0.9	2.9 ± 0.4
14	2-nitrophenyl	3.5 ± 0.8	8.4 ± 0.9	10.4 ± 0.7	4.8 ± 1.7
15	4-nitrophenyl	2.3 ± 0.9	13.7 ± 4.2	12.9 ± 1.4	5.9 ± 2.0
16	1-naphthyl	1.8 ± 0.7	7.8 ± 1.6	7.5 ± 1.5	4.9 ± 0.9
17	2-naphthyl	1.7 ± 0.7	8.8 ± 1.3	7.8 ± 2.3	6.3 ± 0.4

Table 3
Growth inhibition of Mannich Bases 18–27 against carcinoma cell lines. GI50 values are presented as the mean ± sem (standard error of the mean) from four to six separated experiments.

Entry	GI^a_{50} (μM)			
	HeLa	BT483	SKHep	CE81T
18	5.8 ± 0.2	6.5 ± 2.0	26.8 ± 2.6	8.8 ± 2.0
19	1.6 ± 0.4	5.8 ± 1.4	2.6 ± 0.1	2.8 ± 0.7
20	1.4 ± 0.3	8.1 ± 1.1	3.6 ± 0.6	6.7 ± 0.1
21	ND	ND	ND	ND
22	23.0 ± 2.2	28.5 ± 3.4	ND	ND
23	16.9 ± 3.2	ND	ND	ND
24	3.13 ± 0.5	5.7 ± 0.9	15.1 ± 2.8	3.7 ± 1.1
25	0.7 ± 0.3	1.9 ± 0.1	14.6 ± 0.6	5.9 ± 0.5
26	1.2 ± 0.1	11.2 ± 1.5	15.3 ± 1.5	2.8 ± 0.4
27	4.2 ± 1.3	7.1 ± 1.1	5.5 ± 0.6	4.4 ± 1.4

A

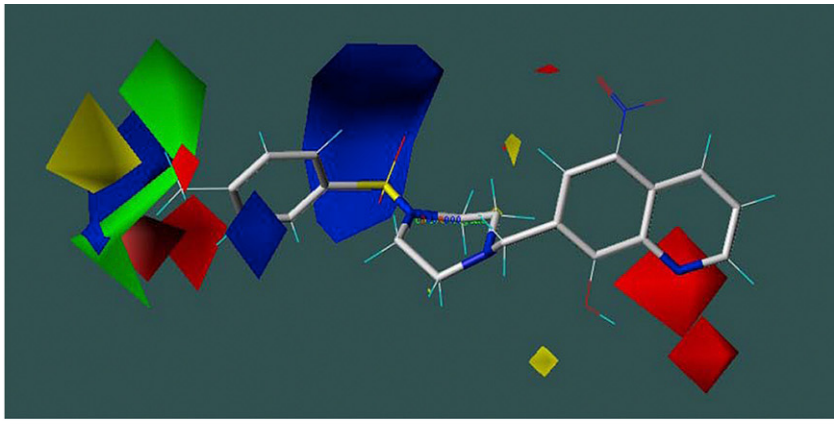

B

Compd	pIC_{50}	Training set	Pred-1	Pred-2	Pred-3	Pred-4
02	5.357	5.267	5.292	5.288	5.328	5.309
03	5.337	5.289	5.422	5.289	5.295	5.286
04	5.168	5.278	**5.491**	5.251	5.266	5.236
05	5.602	5.604	**5.663**	5.619	5.560	5.615
06	5.215	5.204	5.217	5.218	5.202	5.220
07	5.328	5.387	5.326	**5.472**	5.367	5.359
08	5.349	5.406	5.387	5.399	**5.207**	5.389
09	5.658	5.654	5.689	**5.576**	5.684	5.667
10	5.620	5.574	5.649	5.632	5.603	**5.232**
11	5.301	5.301	5.284	5.256	**5.006**	5.306
12	5.310	5.355	**5.711**	5.331	5.329	5.290
13	5.367	5.288	5.350	**5.080**	5.349	5.334
14	5.456	5.521	5.492	5.518	5.560	5.506
15	5.638	5.626	5.627	5.663	5.626	5.634
16	5.745	5.751	5.752	5.752	5.768	5.767
17	5.770	5.690	5.737	5.721	5.673	**5.513**
18	5.237	5.189	5.211	5.175	5.189	5.182
19	5.796	5.841	5.860	5.812	5.788	5.861
20	5.854	5.829	5.825	5.813	5.885	5.825
21	4.222	4.300	4.278	4.290	4.270	4.238
22	4.638	4.595	4.593	4.606	4.587	4.611
23	4.772	4.712	4.729	4.722	4.754	4.758
24	5.505	5.651	5.593	5.616	**5.790**	5.565
25	6.155	6.096	6.082	6.109	6.111	6.076
26	5.921	5.931	5.890	5.931	5.962	5.889
27	5.377	5.352	5.327	5.328	5.382	**5.304**
parameter						
q^2		0.396	0.404	0.408	0.458	0.436
ONC		6	6	6	6	6
STE		0.070	0.054	0.060	0.056	0.048
R^2		0.978	0.989	0.986	0.988	0.991
F value		139.989	229.652	188.009	216.890	283.566
Fraction						
steric		0.525	0.537	0.512	0.519	0.539
electrostatic		0.475	0.463	0.488	0.481	0.461

Fig. 4. 3D-QSAR analysis on HeLa cell line. (A) Steric and electrostatic fields generated with the CoMFA model projected on **25**: yellow indicates regions where bulky groups decrease activity (contribution level of 80%) whereas green indicates regions where bulky groups increase activity (contribution level of 20%); red indicates regions where negatively charged groups increase activity (contribution level of 20%), whereas blue indicates regions where positively charged groups increase activity (contribution level of 80%). The core used in alignment protocol of Sybyl 8.1 program is specified in ball and stick. (B) Statistics of CoMFA analysis.

nitro and methyl groups are correctly positioned into the red (favor negative charge) and blue (favor positive charge) contours (data not shown). On the right side of Fig. 4A, the red contours imply that a negatively charged nitrogen atom in a fused ring system is essential to the growth inhibition. This finding explains why **21**, **22**, and **23**, which are lack of such a property, are ranked the poorest ones along the HeLa column in Table 3. In addition, 5-nitro group para to the 8-hydroxyl group within this fused ring system is a plus contribution as indicated by a small red contour. Accordingly, **25** outperforms **5** and **26** outperforms **15**.

5. Conclusion

In summary, a series of 8-hydroxyquinoline-derived Mannich bases were synthesized and examined for their growth inhibition with interesting SAR results. The structural modifications reveal that 8-hydroxyquinol skeleton is required for activity. All Mannich bases exhibited moderate to low micromolar potency against four carcinoma cells. In particular, **25** showed the most activities against both HeLa and BT483 cells with GI_{50} values of 0.7 and 1.9 μM, respectively, while **19** (GI_{50}, 2.6 and 2.8 μM against SKHep and

CE81T cells, respectively) and **26** (GI_{50}, 2.8 μM against CE81T cells) exhibited the most potent growth-inhibitory effect on SKHep and CE81T cells. These results suggest the selective sensitivity of individual cell lines in response to the tested compounds. Further CoMFA model of 3D-QSAR analysis provided a q^2 value of 0.396 and revealed that both steric and electronic effects are equally significant for activity. Taken together, the structure-activity relationships received from both *in vitro* growth inhibition data and CoMFA model warrant a valuable platform for more detailed study.

6. Experimental protocols

6.1. Synthesis

Chemical reagents and organic solvents were purchased from Acros, Aldrich and Alfa Aesar unless otherwise mentioned. Melting points were determined by Fargo MP-2D. Nuclear magnetic resonance spectra (^{1}H and ^{13}C NMR) were measured on a Bruker AC-300 instrument. Chemical shifts (δ) are reported in ppm relative to the TMS peak. Mass spectra were obtained by FAB on a Jeol JMS-700 instrument. Flash column chromatography was performed with silica gel (230–400 mesh). Elemental Analysis was carried out on a Heraeus VarioEL- III C, H, N analyzer.

6.1.1. General procedure

To a solution of 8-hydroxyquinoline or 1-naphthol (1.05 mmol) and paraformaldehyde (36 mg, 1.26 mmol) in dry ethanol (8 mL) was added the appropriate secondary amine (1.26 mmol) at room temperature. The resulting mixture was heated at reflux for 18–22 h. The solvent was removed *in vacuo* and the crude product was purified by flash chromatography and/or recrystallization [15].

6.1.2. 7-((4-(4-Fluorophenylsulfonyl)piperazin-1-yl)methyl) quinolin-8-ol (**2**)

M.p. 153.2–155.2 °C. ^{1}H NMR (300 MHz, $CDCl_3$) δ 2.69 (m, 4H), 3.08 (m, 4H), 3.85 (s, 2H), 7.20 (s, 2H), 7.25 (m, 2H), 7.38 (dd, J = 8.4, 4.2 Hz, 1H), 7.75 (m, 2H), 8.08 (dd, J = 8.4, 1.7 Hz, 1H), 8.80 (dd, J = 4.2, 1.7 Hz, 1H) ppm. ^{13}C NMR (75 MHz, $CDCl_3$) δ 46.2, 51.9, 58.7, 116.5, 116.8, 117.7, 117.8, 121.7, 128.5, 130.6, 130.7, 131.6, 136.0, 139.0, 148.9, 152.0 ppm. HRMS $(M)^+$ calcd for $C_{20}H_{20}FN_3O_3S$ 401.1209, found 401.1211.

6.1.3. 7-((4-(4-Chlorophenylsulfonyl)piperazin-1-yl)methyl) quinolin-8-ol (**3**)

M.p. 157.3–159.3 °C. ^{1}H NMR (300 MHz, MeOH-d_4) δ 2.66 (m, 4H), 3.07 (m, 4H), 3.86 (s, 2H), 7.34 (s, 2H), 7.46 (d, J = 8.2, 4.1 Hz, 1H), 7.64 (d, J = 8.5 Hz, 2H), 7.76 (d, J = 8.5 Hz, 2H), 8.22 (dd, J = 8.2, 1.4 Hz, 1H), 8.76 (dd, J = 4.1, 1.4 Hz, 1H) ppm. ^{13}C NMR (75 MHz, $CDCl_3$) δ 46.2, 51.9, 58.6, 117.7, 117.8, 121.7, 128.5, 129.3, 129.7, 134.0, 135.7, 136.0, 139.0, 139.9, 148.9, 152.0 ppm. HRMS $(M)^+$ calcd for $C_{20}H_{20}ClN_3O_3S$ 417.0914, found 417.0913. Anal. Calcd. for $C_{20}H_{20}ClN_3O_3S$: C, 57.48; H, 4.82; N, 10.05. Found: C, 57.36; H, 4.64; N, 9.92.

6.1.4. 7-((4-(4-Bromophenylsulfonyl)piperazin-1-yl)methyl) quinolin-8-ol (**4**)

M.p. 188.7–190.7 °C. ^{1}H NMR (300 MHz, $CDCl_3$) δ 2.70 (m, 4H), 3.08 (m, 4H), 3.86 (s, 2H), 7.26 (s, 2H), 7.39 (dd, J = 8.4, 4.2 Hz, 1H), 7.60 (d, J = 8.6 Hz, 2H), 7.68 (d, J = 8.6 Hz, 2H), 8.09 (dd, J = 8.4, 1.5 Hz, 1H), 8.81 (dd, J = 4.2, 1.5 Hz, 1H) ppm. ^{13}C NMR (75 MHz, $CDCl_3$) δ 46.2, 51.9, 58.5, 117.7, 117.8, 119.5, 121.7, 128.4, 128.5, 129.4, 132.6, 134.4, 135.9, 138.9, 148.8, 152.0 ppm. HRMS $(M)^+$ calcd for $C_{20}H_{20}BrN_3O_3S$ 461.0409, found 461.0407. Anal. Calcd. for $C_{20}H_{20}BrN_3O_3S$: C, 51.66; H, 4.59; N, 8.69. Found: C, 51.69; H, 4.55; N, 8.58.

6.1.5. 7-((4-Tosylpiperazin-1-yl)methyl)quinolin-8-ol (**5**)

M.p. 161.6–163.6 °C. ^{1}H NMR (300 MHz, $CDCl_3$) δ 2.44 (s, 3H), 2.69 (m, 4H), 3.05 (m, 4H), 3.85 (s, 2H), 7.23 (s, 1H), 7.24 (s, 1 H), 7.32 (d, J = 8.2 Hz, 2H), 7.37 (dd, J = 8.4, 4.2 Hz, 1H), 7.61 (d, J = 8.2 Hz, 2H), 8.07 (dd, J = 8.4,1.5 Hz, 1H), 8.80 (dd, J = 4.2, 1.5 Hz, 1H) ppm. ^{13}C NMR (75 MHz, $CDCl_3$) δ 21.7, 46.3, 51.9, 59.1, 117.6, 117.8, 121.6, 128.0, 128.3, 128.5, 129.9, 132.1, 135.9, 139.1, 144.1, 148.9, 152.3 ppm. HRMS $(M)^+$ calcd for $C_{21}H_{23}N_3O_3S$ 397.1460, found 397.1459. Anal. Calcd. for $C_{21}H_{23}N_3O_3S$: C, 57.48; H, 4.82; N, 10.05. Found: C, 57.20; H, 4.61; N, 10.26.

6.1.6. 7-((4-(4-Isopropylphenylsulfonyl)piperazin-1-yl)methyl) quinolin-8-ol (**6**)

M.p. 153.8–155.8 °C. ^{1}H NMR (300 MHz, $CDCl_3$) δ 1.28 (s, 3H), 1.30 (s, 3H), 2.69 (m, 4H), 2.99 (m, 1H), 3.07 (m, 4H), 3.85 (s, 2H), 7.22 (s, 1H), 7.23 (s, 1H), 7.35 (dd, J = 8.2, 4.2 Hz, 1 H), 7.37 (d, J = 8.3 Hz, 2H), 7.64 (d, J = 8.3 Hz, 2H), 8.07 (dd, J = 8.2, 1.6 Hz, 1H), 8.80 (dd, J = 4.2, 1.6 Hz, 1H) ppm. ^{13}C NMR (75 MHz, $CDCl_3$) δ 23.8, 34.4, 46.3, 52.0, 59.2, 117.6, 117.8, 121.7, 127.4, 128.1, 128.3, 128.5, 132.5, 135.9, 139.1, 149.0, 152.3, 154.7 ppm. HRMS $(M)^+$ calcd for $C_{23}H_{27}N_3O_3S$ 425.1773, found 425.1775.

6.1.7. 7-((4-(4-Tert-butylphenylsulfonyl)piperazin-1-yl)methyl) quinolin-8-ol (**7**)

M.p. 184.1–186.1 °C. ^{1}H NMR (300 MHz, $CDCl_3$) δ 1.37 (s, 9H), 2.71 (m, 4H), 3.09 (m, 4H), 3.86 (s, 2H), 7.25 (m, 2H), 7.37 (dd, J = 8.3, 4.2 Hz, 1H), 7.54 (d, J = 8.6 Hz, 2H), 7.65 (d, J = 8.6 Hz, 2H), 8.08 (dd, J = 8.3, 1.6 Hz, 1H), 8.81 (dd, J = 4.2, 1.6 Hz, 1H) ppm. ^{13}C NMR (75 MHz, $CDCl_3$) δ 31.2, 35.4, 46.2, 52.0, 59.2, 117.6, 117.8, 121.7, 126.3, 127.9, 128.3, 128.5, 132.1, 135.9, 139.1, 148.9, 152.3, 157.0 ppm. HRMS $(M)^+$ calcd for $C_{24}H_{29}N_3O_3S$ 439.1930, found 439.1923. Anal. Calcd. for $C_{24}H_{29}N_3O_3S$: C, 61.63; H, 5.76; N, 9.80. Found: C, 61.34; H, 5.75; N, 9.61.

6.1.8. 7-((4-(Biphenyl-4-ylsulfonyl)piperazin-1-yl)methyl)quinolin-8-ol (**8**)

M.p. 225.6–227.6 °C. ^{1}H NMR (300 MHz, $CDCl_3$) δ 2.73 (m, 4H), 3.14 (m, 4H), 3.87 (s, 2H), 7.25 (s, 1H), 7.26 (s, 1H), 7.37 (dd, J = 8.4, 4.2 Hz, 1H), 7.48 (m, 3H), 7.62 (m, 2H), 7.73 (d, J = 8.4 Hz, 2H), 7.80 (d, J = 8.4 Hz, 2H), 8.08 (dd, J = 8.4, 1.7 Hz, 1H), 8.80 (dd, J = 4.2, 1.7 Hz, 1H) ppm. ^{13}C NMR (75 MHz, $CDCl_3$) δ 46.3, 52.0, 59.0, 87.2, 117.6, 117.8, 121.7, 127.6, 128.0, 128.5, 128.7, 129.2, 133.7, 135.7, 135.9, 139.0, 139.5, 146.3, 148.9, 152.2 ppm. HRMS $(M)^+$ calcd for $C_{26}H_{25}N_3O_3S$ 459.1617, found 459.1620. Anal. Calcd. for $C_{26}H_{25}N_3O_3S$: C, 67.95; H, 5.48; N, 9.14. Found: C, 67.73; H, 5.69; N, 9.41.

6.1.9. 7-((4-(4-(Trifluoromethyl)phenylsulfonyl)piperazin-1-yl) methyl)quinolin-8-ol (**9**)

M.p. 168.3–170.3 °C. ^{1}H NMR (300 MHz, $CDCl_3$) δ 2.68 (m, 4H), 3.09 (m, 4H), 3.83 (s, 2H), 7.24 (s, 2H), 7.36 (dd, J = 8.4, 4.2 Hz, 1H), 7.79 (d, J = 8.5 Hz, 2H), 7.85 (d, J = 8.5 Hz, 2H), 8.07 (dd, J = 8.4, 1.5 Hz, 1H), 8.78 (dd, J = 4.2, 1.5 Hz, 1H) ppm. ^{13}C NMR (75 MHz, $CDCl_3$) δ 46.2, 51.9, 58.4, 117.6, 117.8, 121.7, 126.4, 126.4, 126.5, 126.5, 128.4, 128.6, 135.9, 138.8, 139.1, 148.8, 151.9 ppm. HRMS (M)+ calcd for $C_{21}H_{20}F_3N_3O_3S$ 451.1177, found 451.1186. Anal. Calcd. for $C_{21}H_{20}F_3N_3O_3S$: C, 55.87; H, 4.47; N, 9.31. Found: C, 55.83; H, 4.23; N, 9.21.

6.1.10. 7-((4-(3-Methoxyphenylsulfonyl)piperazin-1-yl)methyl) quinolin-8-ol (**10**)

M.p. 122.1–124.1 °C. ^{1}H NMR (300 MHz, $CDCl_3$) δ 2.71 (m, 4H), 3.10 (m, 4H), 3.85 (s, 2H), 3.86 (s, 3H),7.15 (m, 1H), 7.24 (m, 1H), 7.30 (m, 2H), 7.37 (dd, J = 8.4, 4.2 Hz, 1H), 7.42 (m, 2H), 8.08 (dd, J = 8.4, 1.5 Hz, 1H), 8.82 (dd, J = 4.2, 1.5 Hz, 1H) ppm. ^{13}C NMR (75 MHz,

$CDCl_3$) δ 46.2, 51.9, 55.8, 59.0, 112.9, 117.6, 117.8, 119.2, 120.0, 121.6, 128.3, 128.4, 130.3, 135.9, 136.3, 139.0, 148.9, 152.2, 160.1 ppm. HRMS $(M)^+$ calcd for $C_{21}H_{23}N_3O_4S$ 413.1409, found 413.1411.

*6.1.11. 7-((4-(4-Methoxyphenylsulfonyl)piperazin-1-yl)methyl) quinolin-8-ol (**11**)*

M.p. 182.3–184.3 °C. ^{1}H NMR (300 MHz, $CDCl_3$) δ 2.70 (brs, 4H), 3.06 (brs, 4H), 3.86 (s, 2H), 3.89 (s, 3H), 7.00 (d, J = 8.7 Hz, 2H), 7.24 (s, 2H), 7.37 (dd, J = 8.4, 4.2 Hz, 1H), 7.67 (d, J = 8.7 Hz, 2H), 8.08 (dd, J = 8.4, 1.5 Hz, 1H), 8.81 (dd, J = 4.2, 1.5 Hz, 1H) ppm. ^{13}C NMR (75 MHz, $CDCl_3$) δ 46.3, 52.0, 55.9, 59.2, 114.5, 117.6, 117.9, 121.7, 126.7, 128.3, 128.5, 130.1, 135.9, 139.1, 149.0, 152.4, 163.4 ppm. HRMS $(M+1)^+$ calcd for $C_{21}H_{24}N_3O_4S$ 414.1488, found 414.1488.

*6.1.12. 7-((4-(3,4-Dimethoxyphenylsulfonyl)piperazin-1-yl)methyl) quinolin-8-ol (**12**)*

M.p. 81.5–83.5 °C. ^{1}H NMR (300 MHz, $CDCl_3$) δ 2.71 (m, 4H), 3.08 (m, 4H), 3.86 (s, 2H), 3.92 (s, 3H), 3.97 (s, 3H), 6.97 (d, J = 8.4 Hz, 1H), 7.18 (d, J = 2.1 Hz, 1H), 7.24 (m, 2H), 7.32 (dd, J = 8.4, 2.1 Hz, 1H), 7.37 (dd, J = 8.4, 4.2 Hz, 1H), 8.08 (dd, J = 8.4, 1.5 Hz, 1H), 8.81 (dd, J = 4.2, 1.5 Hz, 1H) ppm. ^{13}C NMR (75 MHz, $CDCl_3$) δ 46.3, 52.0, 56.4, 59.1, 110.4, 110.9, 117.6, 117.9, 121.7, 121.9, 126.8, 128.3, 128.5, 135.9, 139.0, 149.0, 149.3, 152.3, 153.1 ppm. HRMS $(M)^+$ calcd for $C_{22}H_{25}N_3O_5S$ 443.1515, found 443.1516. Anal. Calcd. for $C_{22}H_{25}N_3O_5S$: C, 59.58; H, 5.68; N, 9.47. Found: C, 59.42; H, 5.55; N, 9.27.

*6.1.13. 7-((4-(4-(Trifluoromethoxy)phenylsulfonyl)piperazin-1-yl) methyl)quinolin-8-ol (**13**)*

M.p. 145.6–147.6 °C. ^{1}H NMR (300 MHz, $CDCl_3$) δ 2.70 (m, 4H), 3.10 (m, 4H), 3.86 (s, 2H), 7.26 (m, 2H), 7.34 (d, J = 6.9 Hz, 2H), 7.36 (dd, J = 8.4, 4.2 Hz, 1H), 7.79 (d, J = 6.9 Hz, 2H), 8.09 (dd, J = 8.4, 1.5 Hz, 1H), 8.81 (dd, J = 4.2, 1.5 Hz, 1H) ppm. ^{13}C NMR (75 MHz, $CDCl_3$) δ 46.2, 52.0, 58.6, 117.7, 117.9, 121.2, 121.8, 128.4, 128.6, 130.1, 134.0, 136.0, 139.0, 148.9, 152.0, 152.7 ppm. HRMS $(M)^+$ calcd for $C_{21}H_{20}F_3N_3O_4S$ 467.1127, found 467.1130.

*6.1.14. 7-((4-(2-Nitrophenylsulfonyl)piperazin-1-yl)methyl) quinolin-8-ol (**14**)*

M.p. 78.6–80.6 °C. ^{1}H NMR (300 MHz, $CDCl_3$) δ 2.70 (t, J = 5.0 Hz, 4H), 3.37 (t, J = 5.0 Hz, 4H), 3.88 (s, 2H), 7.29 (m, 2H), 7.40 (dd, J = 8.4, 4.2 Hz, 1H), 7.61 (m, 1H), 7.70 (m, 2H), 7.92 (m, 1H), 8.10 (dd, J = 8.4, 1.5 Hz, 1H), 8.82 (dd, J = 4.2, 1.5 Hz, 1H) ppm. ^{13}C NMR (75 MHz, $CDCl_3$) δ 46.2, 52.2, 58.7, 117.7, 117.9, 121.7, 124.2, 128.4, 128.6, 130.6, 131.0, 131.6, 134.1, 136.0, 138.9, 148.9, 152.0 ppm. HRMS $(M)^+$ calcd for $C_{20}H_{20}N_4O_5S$ 428.1154, found 428.1149. Anal. Calcd. for $C_{20}H_{20}N_4O_5S$: C, 56.06; H, 4.70; N, 13.08. Found: C, 56.09; H, 5.00; N, 13.34.

*6.1.15. 7-((4-(4-Nitrophenylsulfonyl)piperazin-1-yl)methyl) quinolin-8-ol (**15**)*

M.p. 171.8–173.8 °C. ^{1}H NMR (300 MHz, $CDCl_3$) δ 2.70 (m, 4H), 3.14 (m, 4H), 3.85 (s, 2H), 7.28 (m, 2H), 7.40 (dd, J = 8.4, 4.2 Hz, 1H), 7.93 (d, J = 8.8 Hz, 2H), 8.10 (dd, J = 8.4, 1.5 Hz, 1H), 8.39 (d, J = 8.8 Hz, 2H), 8.80 (dd, J = 4.2, 1.5 Hz, 1H) ppm. ^{13}C NMR (75 MHz, $CDCl_3$) δ 46.2, 51.9, 58.2, 117.6, 117.8, 121.8, 124.5, 128.3, 128.7, 129.0, 136.0, 138.8, 141.6, 148.8, 150.4, 151.8 ppm. HRMS $(M)^+$ calcd for $C_{20}H_{20}N_4O_5S$ 428.1154, found 428.1155. Anal. Calcd. for $C_{20}H_{20}N_4O_5S$: C, 56.06; H, 4.70; N, 13.08. Found: C, 55.89; H, 4.79; N, 13.12.

*6.1.16. 7-((4-(Naphthalen-1-ylsulfonyl)piperazin-1-yl)methyl) quinolin-8-ol (**16**)*

M.p. 84.2–86.2 °C. ^{1}H NMR (300 MHz, $CDCl_3$) δ 2.65 (t, J = 4.9 Hz, 4H), 3.23 (t, J = 4.9 Hz, 4H), 3.81 (s, 2 H), 7.24 (s, 2H), 7.37 (m, 1H), 7.59 (m, 3H), 7.94 (m, 1H), 8.08 (m, 2H), 8.18 (m, 1H), 8.79 (m, 2H) ppm. ^{13}C NMR (75 MHz, $CDCl_3$) δ 45.9, 52.2, 58.6, 117.7, 121.6, 124.3, 125.3, 127.0, 128.3, 128.5, 129.1, 129.2, 130.7, 132.3, 134.5, 134.8, 135.9, 138.9, 148.7, 151.9 ppm. HRMS $(M+1)^+$ calcd for $C_{24}H_{24}N_3O_3S$ 434.1538, found 434.1537.

*6.1.17. 7-((4-(Naphthalen-2-ylsulfonyl)piperazin-1-yl)methyl) quinolin-8-ol (**17**)*

M.p. 201.9–203.9 °C. ^{1}H NMR (300 MHz, $CDCl_3$) δ 2.70 (t, J = 4.9 Hz, 4H), 3.16 (brs, 4H), 3.84 (s, 2 H), 7.24 (s, 2H), 7.36 (dd, J = 8.4, 4.2 Hz, 1H), 7.67 (m, 3H), 7.97 (m, 3H), 8.07 (dd, J = 8.4, 1.5 Hz, 1H), 8.32 (m, 1H), 8.78 (dd, J = 4.2, 1.5 Hz, 1H) ppm. ^{13}C NMR (75 MHz, $CDCl_3$) δ 46.3, 51.9, 58.5, 117.7, 121.5, 122.9, 127.7, 128.0, 128.2, 128.4, 129.0, 129.2, 129.3, 129.4, 132.2, 132.4, 135.0, 135.8, 138.8, 148.7, 151.9 ppm. HRMS $(M)^+$ calcd for $C_{24}H_{23}N_3O_3S$ 433.1460, found 433.1456.

*6.1.18. (4-((8-Hydroxyquinolin-7-yl)methyl)piperazin-1-yl) (phenyl)methanone (**18**)*

^{1}H NMR (300 MHz, $CDCl_3$) δ 2.47 (m, 4H), 3.77 (m, 4H), 7.20 (m, 2H), 7.27 (m, 6H), 7.30 (dd, J = 8.4, 4.2 Hz, 1H), 8.00 (dd, J = 8.4, 1.5 Hz, 1H), 8.74 (dd, J = 4.1, 1.5 Hz, 1H) ppm. ^{13}C NMR (75 MHz, $CDCl_3$) δ 47.4, 52.7, 58.5, 117.5, 117.7, 121.3, 126.9, 128.1, 128.3, 129.5, 129.6, 135.4, 135.7, 138.6, 148.4, 151.7, 170.1 ppm. HRMS $(M)^+$ calcd for $C_{21}H_{21}N_3O_2$ 347.1634, found 347.1638.

*6.1.19. 7-((4-Benzylpiperazin-1-yl)methyl)quinolin-8-ol (**19**)*

M.p. 131.7–133.7 °C. ^{1}H NMR (300 MHz, $CDCl_3$) δ 2.65 (brs, 4H), 2.76 (brs, 4H), 3.60 (s, 2H), 3.96 (s, 2H), 7.31 (m, 5H), 7.39 (dd, J = 8.4, 4.2 Hz, 1H), 8.10 (d, J = 8.4 Hz, 1H), 8.41 (brs, 3H), 8.87 (d, J = 4.2 Hz, 1H) ppm. ^{13}C NMR (75 MHz, $CDCl_3$) δ 52.3, 52.4, 59.7, 62.7, 117.4, 117.7, 121.6, 127.6, 128.3, 128.5, 128.7, 129.6, 136.1, 137.0, 139.1, 149.0, 153.1 ppm. HRMS $(M)^+$ calcd for $C_{21}H_{23}N_3O$ 333.1841, found 333.1850.

*6.1.20. N-(2-((8-Hydroxyquinolin-7-yl)methylamino)ethyl) benzenesulfonamide (**20**)*

M.p. 147.6–149.6 °C. ^{1}H NMR (300 MHz, $CDCl_3$) δ 2.90 (t, J = 6.4 Hz, 2H), 3.42 (t, J = 6.4 Hz, 2H), 3.78 (s, 2H), 4.14 (s, 2H), 7.28 (s, 2H), 7.43 (dd, J = 8.1, 4.3 Hz, 1H), 7.53 (d, J = 7.4 Hz, 2H), 7.61 (m, 1H), 7.85 (d, J = 7.4 Hz, 2H), 8.13 (d, J = 8.1, 1H), 8.79 (d, J = 4.3 Hz, 1H) ppm. ^{13}C NMR (75 MHz, $CDCl_3$) δ 45.7, 52.0, 52.5, 70.3, 117.8, 118.7, 121.9, 127.8, 128.1, 129.0, 129.3, 133.1, 136.1, 137.4, 138.5, 148.5, 150.6 ppm. HRMS $(M)^+$ calcd for $C_{18}H_{19}N_3O_3S$ 357.1147, found 357.1143. Anal. Calcd. for $C_{18}H_{19}N_3O_3S$: C, 60.49; H, 5.36; N, 11.76. Found: C, 61.57; H, 5.26; N, 11.38.

*6.1.21. 2-((4-(Phenylsulfonyl)piperazin-1-yl)methyl)phenol (**21**)*

M.p. 151.6–153.6 °C. ^{1}H NMR (300 MHz, $CDCl_3$) δ 2.64 (brs, 4H), 3.09 (brs, 4H), 3.70 (s, 2H), 6.77 (m, 2H), 6.97 (m, 1H), 7.16 (m, 1H), 7.59 (m, 3H), 7.75 (m, 2H), 10.08 (brs, 1H) ppm. ^{13}C NMR (75 MHz, $CDCl_3$) δ 46.1, 51.8, 61.2, 116.2, 119.7, 120.6, 127.9, 129.1, 129.3, 129.4, 133.4, 135.5, 157.3 ppm. HRMS $(M)^+$ calcd for $C_{17}H_{20}N_2O_3S$ 332.1195, found 332.1191.

*6.1.22. 2-((4-(Phenylsulfonyl)piperazin-1-yl)methyl)pyridin-3-ol (**22**)*

M.p. 146.1–148.1 °C. ^{1}H NMR (300 MHz, $CDCl_3$) δ 2.71 (brs, 4H), 3.14 (brs, 4H), 3.92 (s, 2H), 7.04 (d, J = 8.2 Hz, 1H), 7.10 (dd, J = 8.2, 6.1 Hz, 1H), 7.57 (d, J = 8.7 Hz, 2H), 7.65 (m, 1H), 7.76 (dd, J = 8.7, 2H), 8.03 (d, J = 6.1, 1H) ppm. ^{13}C NMR (75 MHz, $CDCl_3$) δ 45.9, 52.0, 63.4, 123.1, 124.0, 127.8, 129.4, 133.4, 135.6, 140.6, 141.6, 153.9 ppm. HRMS $(M)^+$ calcd for $C_{16}H_{19}N_3O_3S$ 333.1147, found 333.1150. Anal. Calcd. for $C_{16}H_{19}N_3O_3S$: C, 57.64; H, 5.74; N, 12.60. Found: C, 57.58; H, 5.79; N, 12.44.

*6.1.23. 2-((4-(Phenylsulfonyl)piperazin-1-yl)methyl)naphthalen-1-ol(**23**)*

M.p. 92.0–94.0 °C. ^{1}H NMR (300 MHz, $CDCl_3$) δ 2.71 (brs, 4H), 3.11 (brs, 4H), 3.85 (s, 2H), 7.05 (d, J = 8.4 Hz, 1H), 7.29 (d, J = 8.4 Hz, 1H), 7.43 (m, 2H), 7.57 (d, J = 7.9 Hz, 2H), 7.65 (d, J = 6.9 Hz, 1H), 7.75 (d, J = 7.9 Hz, 2 H), 7.77 (m, 1H), 8.11 (t, J = 6.9 Hz, 1H) ppm. ^{13}C NMR (75 MHz, $CDCl_3$) δ 46.1, 51.9, 61.3, 113.0, 119.0, 122.4, 125.1, 126.4, 126.7, 127.6, 127.7, 127.9, 129.5, 133.4, 134.2, 135.7, 153.0 ppm. HRMS $(M)^+$ calcd for $C_{21}H_{22}N_2O_3S$ 382.1351, found 382.1350.

*6.1.24. 5-Nitro-7-((4-(Phenylsulfonyl)piperazin-1-yl)methyl) quinolin-8-ol (**24**)*

M.p. 132.7–134.7 °C. ^{1}H NMR (300 MHz, $CDCl_3$) δ 2.73 (t, J = 4.8 Hz, 4H), 3.11 (t, J = 4.8 Hz, 4H), 3.89 (s, 2H), 7.55 (m, 1H), 7.57 (d, J = 7.2 Hz, 2H), 7.63 (dd, J = 8.8, 3.1 Hz, 1 H), 7.67 (m, 1H), 7.75 (d, J = 7.2 Hz, 2H), 8.46 (s, 1H), 8.91 (d, J = 3.1 Hz, 1H), 9.26 (d, J = 8.8 Hz, 1H) ppm. ^{13}C NMR (75 MHz, $CDCl_3$) δ 46.1, 52.1, 57.3, 116.7, 122.3, 125.0, 127.9, 129.2, 129.4, 133.4, 135.4, 135.7, 136.0, 137.8, 149.6, 158.3 ppm. HRMS $(M+1)^+$ calcd for $C_{20}H_{21}N_4O_5S$ 429.1233, found 429.1239.

*6.1.25. 5-Nitro-7-((4-(4-Nitrophenylsulfonyl)piperazin-1-yl) methyl)quinolin-8-ol (**26**)*

M.p. 224.6–226.6 °C. ^{1}H NMR (300 MHz, d_6-DMSO) δ 2.48 (brs, 4H), 2.90 (brs, 4H), 3.62 (s, 2H), 7.45 (m, 1H), 7.96 (d, J = 8.5 Hz, 2H), 8.13 (m, 1H), 8.43 (d, J = 8.5 Hz, 2H), 8.50 (s, 1H), 9.26 (m, 1H) ppm. ^{13}C NMR (75 MHz, d_6-DMSO) δ 46.0, 51.6, 55.2, 119.6, 124.2, 124.8, 125.1, 129.2, 133.6, 134.5, 139.8, 140.7, 145.1, 150.2, 172.7 ppm. HRMS $(M+1)^+$ calcd for $C_{20}H_{19}N_5O_7S$ 473.1005, found 473.1004.

*6.1.26. 5-Chloro-7-((4-(Phenylsulfonyl)piperazin-1-yl)methyl) quinolin-8-ol (**27**)*

M.p. 155.2–157.2 °C. ^{1}H NMR (300 MHz, $CDCl_3$) δ 2.70 (t, J = 4.8 Hz, 4H), 3.09 (t, J = 4.8 Hz, 4H), 3.82 (s, 2H), 7.36 (s, 1H), 7.49 (m, 1H), 7.56 (d, J = 7.1 Hz, 2H), 7.62 (dd, J = 8.5, 4.2 Hz, 1H), 7.74 (d, J = 7.1 Hz, 2H), 8.46 (d, J = 8.5 Hz, 1H), 8.85 (d, J = 4.2 Hz, 1H) ppm. ^{13}C NMR (75 MHz, $CDCl_3$) δ 46.2, 52.1, 58.3, 118.1, 120.5, 122.5, 126.1, 128.0, 129.4, 133.2, 133.3, 135.3, 139.4, 149.4, 151.3 ppm. HRMS $(M+1)^+$ calcd for $C_{20}H_{21}ClN_3O_3S$ 418.0992, found 418.0999.

6.2. Cell culture

Cancer cells were purchased from Bioresource Collection and Research Center in Taiwan. Each cell line was maintained in the standard medium and grown as a monolayer in Dulbecco's Modified Eagle Medium (DMEM) containing 10% fetal bovine serum, 2 mM glutamine, 100 units/ml penicillin, and 100 g/mL streptomycin. Cultures were maintained at 37 °C with 5% CO_2 in a humidified atmosphere.

6.3. MTT assay for cell viability

Cells were plated in 96-well microtiter plates at a density of 5 x10^3/well and incubated for 24 h. After that, cells were treated with vehicle alone (control) or compounds (drugs were dissolved in DMSO previously) at the concentrations indicated. Treated cells were further incubated for 48 h. Cell survival is expressed as percentage of control cell growth. The 3-[4, 5-Dimethylthiazol-2-yl]-2, 5-diphenyltetrazolium bromide (MTT, 2 mg/mL) dye reduction assay in 96-well microplates was used. The assay is dependent on the reduction of MTT by mitochondrial dehydrogenases of viable cell to a blue formazan product, which come be measured spectrophotometrically. Tumor cells were incubated in each well with serial dilutions of the tested compounds. After 2 days of incubation (37 °C, 5% CO_2 in a humid atmosphere) 100 μL of MTT (2 mg/mL in PBS) was added to each well and the plate was incubated for a further 2 h (37 °C). The resulting formazan was dissolved in 100 μL DMSO and read at 570 nm. The percentage of growth inhibition was calculated by the following equation: percentage growth inhibition = (1 -At/Ac) × 100, where At and Ac represent the absorbance in treated and control cultures, respectively. The drug concentration causing a 50% cell growth inhibition (GI_{50}) was determined by interpolation from dose-response curves. All determinations were carried out in four to six separated experiments.

6.4. Statistical analysis

Data are presented as the mean ± sem (standard error of the mean) from four to six separated experiments. Statistical analyses were performed using Bonferroni *t*-test method after ANOVA for multigroup comparison and Student's *t*-test method for two-group comparison. $P = 0.05$ was considered significant. Analysis of linear regression (at least five data within 20–80% inhibition) was used to calculate GI_{50} value.

Acknowledgments

Financial support from the National Science Council of the Republic of China and Tamkang University to A. Y. Shaw is gratefully acknowledged.

References

[1] K.C. Song, J.S. Kim, S.M. Park, K.-C. Chung, S. Ahn, S.-K. Chang, Org. Lett. 8 (16) (2006) 3413–3416.
[2] H. Zhang, L.-F. Han, K.A. Zachariasse, Y.-B. Jiang, Org. Lett. 7 (19) (2005) 4217–4220.
[3] N.M. Shavaleev, R. Scopelliti, F. Gumy, J.-C.G. Bünzli, Inorg. Chem. 47 (19) (2008) 9055–9068.
[4] T.-T. Wang, G.-C. Zeng, H.-P. Zeng, P.-Y. Liu, R.-X. Wang, Z.-J. Zhang, Y.-L. Xiong, Tetrahedron 65 (32) (2009) 6325–6329.
[5] R.T. Borchardt, D.R. Thakker, J. Med. Chem. 19 (1976) 558–560.
[6] S.A. Saeed, R.U. Simjee, A.H. Gilani, S. Siddiqui, R. Saleem, S. Faizi, B. Siddiqui, S. Farnaz, Biochem. Soc. Trans. 20 (4) (1992) 357S.
[7] L. Zhuang, J.S. Wai, M.W. Embrey, T.E. Fisher, M.S. Egbertson, L.S. Payne, J. P. Guare Jr., J.P. Vacca, D.J. Hazuda, P.J. Felock, A.L. Wolfe, K.A. Stillmock, M. V. Witmer, G. Moyer, W.A. Schleif, L.J. Gabryelski, Y.M. Leonard, J.J. Lynch Jr., S. R. Michelson, S.D. Young, J. Med. Chem. 46 (4) (2003) 453–456.
[8] I. Szabo, Nature 212 (5068) (1966) 1384–1385.
[9] H. Gershon, R. Parmegiani, Appl. Microbiol. 10 (1962) 348–353.
[10] N.A. Negm, S.M.I. Morsy, M.M. Said, Bioorg. Med. Chem. 13 (21) (2005) 5921–5926.
[11] L.W. Scheibel, A. Adler, Mol. Pharmacol. 18 (2) (1980) 320–325.
[12] M. Yamato, K. Hashigaki, Y. Yasumoto, J. Sakai, S. Tsukagoshi, T. Tashiro, T. Tsuruo, Chem. Pharm. Bull. 34 (8) (1986) 3496–3498.
[13] V. Moret, Y. Laras, T. Cresteil, G. Aubert, D.Q. Ping, C. Di, M. Barthélémy-Requin, C. Béclin, V. Peyrot, D. Allegro, A. Rolland, F. De Angelis, E. Gatti, P. Pierre, L. Pasquini, E. Petrucci, U. Testa, J.-L. Kraus, Eur. J. Med. Chem. 44 (2) (2009) 558–567.
[14] R.L. Shriner, G.F. Grillot, W.O. Teeters, J. Am. Chem. Soc. 68 (1946) 946–947.
[15] J.H. Burckhalter, R.I. Leib, J. Org. Chem. 26 (1961) 4078–4083.
[16] M. Medic-Saric, D. Maysinger, M. Movrin, I. Dvorzak, Chemotherapy 26 (4) (1980) 263–267.
[17] B. Murugasu-Oei, T. Dick, Int. J. Antimicrob. Agents 18 (6) (2001) 579–582.
[18] R.A. Cherny, C.S. Atwood, M.E. Xilinas, D.N. Gray, W.D. Jones, C.A. McLean, K. J. Barnham, I. Volitakis, F.W. Fraser, Y. Kim, X. Huang, L.E. Goldstein, R.D. Moir, J. T. Lim, K. Beyreuther, H. Zheng, R.E. Tanzi, C.L. Masters, A.I. Bush, Neuron 30 (2001) 665–676.
[19] C.W. Ritchie, A.I. Bush, A. Mackinnon, S. Macfarlane, M. Mastwyk, L. MacGregor, L. Kiers, R. Cherny, Q.X. Li, A. Tammer, D. Carrington, C. Mavros, I. Volitakis, M. Xilinas, D. Ames, S. Davis, K. Beyreuther, R.E. Tanzi, C.L. Masters, Arch. Neurol. 60 (12) (2003) 1685–1691.
[20] W.-Q. Ding, B. Liu, J.L. Vaught, H. Yamauchi, S.E. Lind, Cancer Res. 65 (8) (2005) 3389–3395.
[21] W.-Q. Ding, H.-J. Yu, S.E. Lind, Cancer Lett. 271 (2008) 251–259.
[22] H.-L. Chen, C.-Y. Chang, H.-T. Lee, H.-H. Lin, P.-J. Lu, C.-N. Yang, C.-W. Shiau, A. Y. Shaw, Bioorg. Med. Chem. 17 (20) (2009) 7239–7247.
[23] T. Mosman, J. Immunol, Methods 65 (1–2) (1983) 55–63.